Effects of a Macroscopic Fixed Charge Inhomogeneity on Some Membrane Transport Properties

SALVADOR MAFÉ, JOSÉ A. MANZANARES, M. JESÚS HERNÁNDEZ, AND JULIO PELLICER[1]

Departamento Termodinámica, Universidad de Valencia, 46100 Burjasot, Spain

Received December 3, 1990; accepted January 29, 1991

The effects that a macroscopic fixed charge inhomogeneity exerts on some membrane transport properties have been theoretically analyzed. To this end, we introduce two particular inhomogeneous fixed charge distributions on the basis of previous experimental work, and the transport equations are assumed to be the Nernst–Planck equations. It is found that a macroscopic redistribution of a constant quantity of fixed charge groups can modify the observed transport properties, the two inhomogeneous membranes here considered exhibiting permselectivities different from those of otherwise identical homogeneous membranes. Although the main emphasis of the study is on the basic aspects of transport through inhomogeneous membranes, some of the conclusions obtained may be of interest for membrane design and application.

INTRODUCTION

It has conclusively been shown that the distribution of the fixed charge groups may be nonuniform on a macroscopic or a microscopic level in many synthetic membranes (see, e.g., (1–4) and references therein). The occurrence of spatial nonuniformities in membrane systems has a number of implications: Reiss and co-workers (1, 2) have shown that an inhomogeneity in the fixed charge distribution can lead to higher current efficiencies than those observed in an otherwise identical homogeneous membrane. Pinéri (3) has pointed out that the membrane exchange properties and the ionic conductivity must strongly depend on the particular fixed charge distribution. Petropoulos (4) has recently published an important paper with some practical examples that clearly point out the need for studying how membrane structural inhomogeneities influence the transport properties. According to this work (4), studying the effects that membrane inhomogeneity exerts on transport properties is of interest because of both the possibility of exploiting such effects in membrane design and the need for a better understanding of the transport processes taking place in supposedly "homogeneous" membranes. Larter and co-workers (5–8) have been able to confirm that the existence of nonlinear transport equations in spatially nonuniform systems can result in significant flux enhancements. Likewise, the effects of a nonuniform charge distribution on the electric potential across biological membranes with surface charge layers have also been examined by Ohshima *et al.* (9).

In this paper we have considered the effects that a fixed charge inhomogeneity on a *macroscopic* scale exerts on some membrane transport properties. We have introduced two particular fixed charge distributions showing some of the results obtained from X-ray microprobe techniques by Pinéri and co-workers (3). According to these measurements, some membranes exhibit a local fixed charge concentration that decreases as we move from the membrane surfaces to the membrane core (some important transient transport properties

[1] To whom correspondence should be addressed.

0021-9797/91 $3.00

of these membranes are mentioned in (4)). Conversely, other membranes have fixed charge values increasing from the membrane surfaces to the membrane interior (3). We will study here how these two macroscopic fixed charge inhomogeneities influence the average coion concentration within the membrane, the membrane resistance, and the ratio between the counterion and the coion fluxes. The membrane models employed are very simple and incorporate a parameter accounting for the membrane inhomogeneity degree. The transport equations are approximately represented by the steady-state Nernst–Planck flux equations. Buck (10) has reviewed the validity of these equations when applied to inhomogeneous systems. Taking into account the macroscopic length scale of the inhomogeneities here dealt with, use of the Nernst–Planck equations seems to be a reasonable first approach to a certainly complex problem (1, 2, 10). Although our study is mainly concerned with the modeling of ionic transport through particular inhomogeneous membranes, some of the conclusions obtained may also be of interest in membrane design and application.

MEMBRANE MODEL AND TRANSPORT EQUATIONS

Figures 1 and 2 show the two membrane models (referred to as models 1 and 2) considered. They correspond respectively to the fixed charge distributions

$$X_1(x) = X_{10}[1 - (1 - 2x/d)^{2n}] \quad [1]$$

and

$$X_2(x) = X_{20}(1/2 + 1/4n)(1 - 2x/d)^{2n} + X_{20}(1/2 - 1/4n), \quad [2]$$

where d is the membrane thickness, $X_i(x)$ the local fixed charge concentration, X_{i0} the maximum value of X_i, and x the spatial coordinate inside the membrane. It is expected that the functions defined in Eqs. [1] and [2] will reproduce some of the experimental trends observed in Ref. (3). Note that parameter n accounts for the membrane inhomogeneity degree (see Figs. 1 and 2). Consider for instance model 1 in Fig. 1. For $n = 2$, we have $X_1(x = 0.08d)/X_{10} = 0.5$ and $X_1(x = 0.22d)/X_{10} = 0.9$. However, the case $n = 10$ leads to $X_1(x = 0.02d)/X_{10} = 0.5$ and $X_1(x = 0.05d)/X_{10} = 0.9$. That is, the membrane inhomogeneity decreases with n, the value $n = \infty$ being that of a homogeneous membrane. In each one of the cases considered later, the *average* fixed charge concentration, $\bar{X}_i$, is taken to be the same regardless the value of n. Thus, the values of X_{i0} are given by

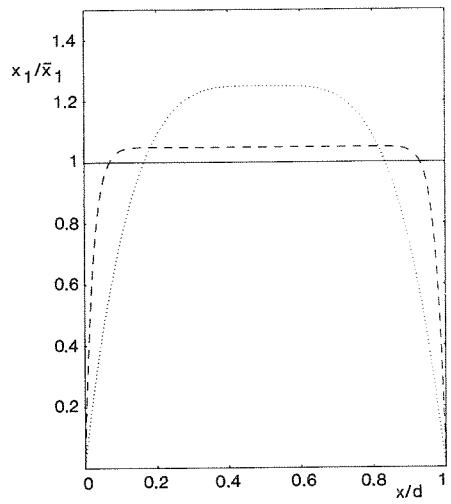

FIG. 1. Membrane model 1 for different values of n: (· · ·) 2, (---) 10, (—) ∞.

$$\bar{X}_1 = \frac{1}{d}\int_0^d X_1(x)dx = \frac{X_{10}}{1 + 1/2n} \quad [3]$$

and

$$\bar{X}_2 = \frac{1}{d}\int_0^d X_2(x)dx = \frac{X_{20}}{2}. \quad [4]$$

This procedure allows for studying which effects are caused just by the redistribution of constant quantities of fixed charge groups. This redistribution is accomplished by considering different values for parameter n.

The basic transport equations describing

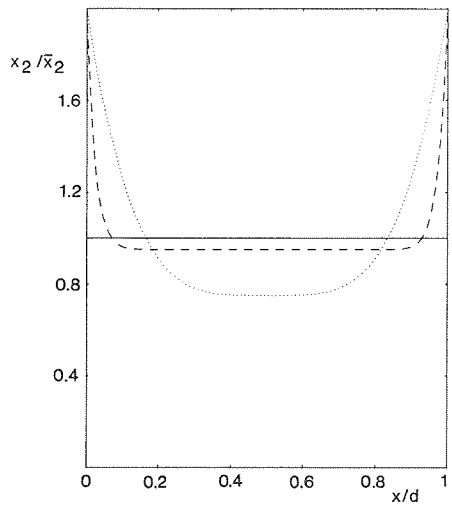

FIG. 2. Membrane model 2 for different values of n: (· · ·) 2, (---) 10, (—) ∞.

our problem are assumed to be the steady-state Nernst–Planck equations for uni-univalent ions

$$J_k = -D_k\left[\frac{dc_k}{dx} + (-1)^{k+1}c_k\frac{d\psi}{dx}\right], \quad k = 1, 2, \quad [5]$$

the local electroneutrality assumption

$$c_1 - c_2 - X = 0, \quad [6]$$

the equation for the electric current density, i,

$$i/F = J_1 - J_2, \quad [7]$$

and the condition of steady-state fluxes

$$dJ_1/dx = 0. \quad [8]$$

Equations [5]–[8] are the basis of many simplified treatments for transport phenomena in charged membranes, and their origin and limitations can be found elsewhere (10). Here J_k, D_k, and c_k denote the flux, the diffusion coefficient, and the local molar concentration of the species k, respectively. On the other hand, ψ stands for the local electric potential in RT/F units. Note that the local electroneutrality assumption, Eq. [6], is introduced instead of the more general Poisson equation. Taking into account that the region where the fixed charge inhomogeneity occurs is *macroscopic* in nature ($d \gg L_D$, L_D being a typical electrolyte Debye length), Eq. [6] can be a reasonable approximation (10).

We further assume that the boundary conditions for the concentrations c_k can be obtained from the following simplified forms of the Donnan equilibrium relationship [1] at the membrane–solution interfaces,

$$c_2(0) = -X_i(0)/2 + [(X_i(0)/2)^2 + c_0^2]^{1/2}, \quad [9]$$

$$c_1(0) = c_2(0) + X_i(0) = c_0^2/c_2(0), \quad [10]$$

$$c_2(d) = -X_i(d)/2 + [(X_i(d)/2)^2 + c_0^2]^{1/2}, \quad [11]$$

$$c_1(d) = c_2(d) + X_i(d) = c_0^2/c_2(d), \quad [12]$$

where c_0 is the bulk solution concentration (the same for the two solutions flanking the membrane). Equations [9]–[12] apply only for model 2 (for model 1 we assume $c_k(0) = c_k(d) = c_0$). In Eqs. [6] and [9]–[12] we have considered, without loss of generality, that the membrane has negative fixed charge groups. It must be mentioned (4, 10) that other mechanisms, in addition to the electric potential difference established between the membrane interior and the solution, can influence the partition equilibrium of species k. Thus, Eqs. [9]–[12] neglect some contributions from the chemical affinity, the swelling pressure, and the activity coefficients and should be regarded as a crude first approximation to the boundary condition problem.

By reordering Eqs. [5]–[6], the following expressions readily follow:

$$\frac{d\psi}{dx} = -\frac{1}{X_i}\times\left(2\frac{dc_2}{dx} + \frac{dX_i}{dx} + \frac{J_1}{D_1} + \frac{J_2}{D_2}\right), \quad [13]$$

$$-\frac{J_2}{D_2} = \frac{dc_2}{dx} + \frac{c_2}{X_i}\left(2\frac{dc_2}{dx} + \frac{dX_i}{dx} + \frac{J_1}{D_1} + \frac{J_2}{D_2}\right), \quad [14]$$

$$\frac{dc_2}{dx} = -\left[c_2\left(\frac{dX_i}{dx} + \frac{J_1}{D_1} + \frac{J_2}{D_2}\right) + X_i\frac{J_2}{D_2}\right]\Big/(2c_2 + X_i). \quad [15]$$

Equations [13]–[15] apply for the two membrane models considered in Figs. 1 and 2 when $n = 2$, 10. In the homogeneous case, Eq. [15] can be solved by analytical methods. To solve them for a given membrane model, we have taken a total number of 2500 points within the membrane. Given a value for the electric current density, i, a nonlinear equation for c_2, Eq. [15], should be solved with the appropriate boundary conditions. To this end, we introduce a guessed value for the flux J_1, and then solve Eq. [15] making use of a fourth-order Runge–Kutta numerical algorithm (11). By comparing the resulting coion concentration at $x = d$ with the actual one, an improved new guess for J_1 is obtained. This procedure is repeated until a previously established convergence is attained. Then, we can solve for the electric potential, $\psi(x)$, and the other magnitudes of interest. The numerical procedure just outlined is very simple and quick (it lasts less than 1 min when implemented on a HP9000/330 computer).

TABLE I

The Different Cases for Which the Set of Differential Equations Is Solved

	$c_0/\bar{X}_i$	D_1/D_2	n	i (mA/cm^2)
Model 1	10^{-2}			
	10^{-1}	10^{-1}	2	1
	1			
			10	5
Model 2	1			
		1	∞	10
	10			

RESULTS

Table I shows schematically all the cases for which Eqs. [1]–[15] have been solved. Other input parameters not included in Table I are $c_0 = 10^{-2}$ M and $d = 10^{-2}$ cm. The membrane transport properties studied for each case are defined as

$$\eta \equiv |J_1/J_2|, \quad [16]$$

$$C \equiv \frac{1}{d}\int_0^d c_2(x)dx, \quad [17]$$

$$R_m \equiv \frac{RT}{F^2}\int_0^d \frac{dx}{D_1c_1 + D_2c_2}. \quad [18]$$

It is clear that the flux ratio, η, and the average coion concentration within the membrane, C (mM), are related to the permselective behavior of the membrane, while R_m (Ω cm^2) would represent the electrical resistance of the solution within the membrane (10). We have used a relatively wide range of $\bar{X}_i$ values. Membrane model 1 is considered from $\bar{X}_1 = 10^{-2}$ to 1 M, while model 2 is used for $\bar{X}_2 = 10^{-3}$ and 10^{-2} M. The following typical values are taken for the ionic diffusion coefficients in the two above mentioned $\bar{X}_i$ ranges: $D_1 = 0.1 \cdot D_2 = 10^{-6}$ cm^2/s (model 1), and $D_1 = D_2 = 10^{-5}$ cm^2/s (model 2). (Note that the counterion diffusion coefficient tends to decrease with increasing electrolyte dilution for charged membranes. This effect is not observed in the case of the coion (4).) Likewise, the three values introduced for i (1, 5, and 10 mA/cm^2) are within the usual experimental range.

Figure 3 shows a typical profile for the dimensionless electric potential, $\psi = (F\phi/RT)$, through the membrane. It is clear that the inhomogeneity in the fixed charge distribution causes the potential profile to deviate from the straight line characteristic of an ohmic drop, in agreement with previous results (2). Like-

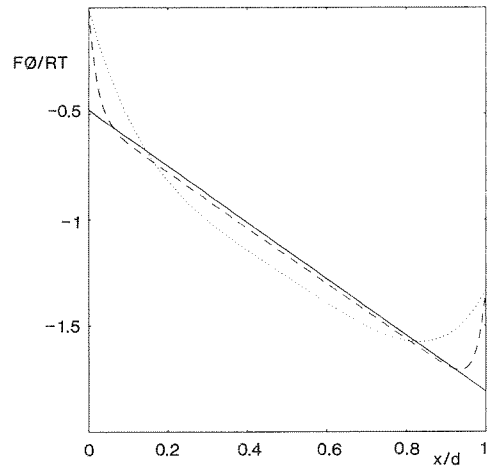

FIG. 3. Electric potential profile across the membrane for model 1. Three different values of parameter n are considered: (· · ·) 2, (---) 10, (—) ∞, being $c_0/\bar{X}_1 = 1$ and $i = 1$ mA/cm^2.

wise, it becomes apparent that the abrupt electric potential jump arising from the application of the Donnan relationship for a homogeneous membrane does not appear in the inhomogeneous membrane simulated by model 1.

On the other hand, Tables II and III contain the values of η, C, and R_m obtained for models 1 and 2, respectively, under the conditions appearing in Table I. Table II corresponds to the membrane model 1, while Table III results from model 2.

Table II shows that the membrane inhomogeneity causes the average coion concentration to take values *greater* than those corresponding to a homogeneous membrane. Petropoulos (4) has considered the effect of a nonuniform distribution of fixed charge groups in the case of microscopic structural inhomogeneities. He has also found that poorer overall coion exclusion generally results. Likewise, the ratio between the counterion and coion fluxes *decreases* when increasing membrane inhomogeneity. These trends are more pronounced for the higher values of the electric current but less pronounced for the higher values of $(c_0/\bar{X}_1)$. Note that when the c_0 values tend to those of $\bar{X}_1$, the fixed charge effects are less pronounced, and then the influence of the membrane inhomogeneity on C and η gradually disappears. Consider now how the inhomogeneous fixed charge distribution affects the electrical resistance R_m. When the fixed charge concentration, $\bar{X}_1$, is high, the resistance, R_m, decreases as the membrane becomes more homogeneous (increasing values of n). Conversely, R_m in-

TABLE II

The Membrane Transport Properties η, C, and R_m Computed for Model 1 Under the Conditions Shown in Table I

		$i = 1$ mA/cm^2			$i = 5$ mA/cm^2			$i = 10$ mA/cm^2		
$\bar{X}_1$ (M)	n	C (mM)	η	R_m ($\Omega \cdot$ cm^2)	C (mM)	η	R_m ($\Omega \cdot$ cm^2)	C (mM)	η	R_m ($\Omega \cdot$ cm^2)
1	2	0.180	556	3.92	0.185	541	3.92	0.201	497	3.91
	10	0.120	862	2.97	0.121	828	2.97	0.123	815	2.97
	∞	0.100	1000	2.66	0.100	1000	2.66	0.100	1000	2.66
10^{-1}	2	1.37	7.40	24.5	2.32	4.41	23.0	4.23	2.46	20.5
	10	1.08	9.32	24.1	1.31	7.71	23.6	1.77	5.76	22.7
	∞	0.990	10.2	24.0	0.990	10.2	24.0	0.990	10.2	24.0
10^{-2}	2	6.33	0.257	33.8	6.94	0.244	31.6	7.97	0.225	28.4
	10	6.22	0.260	34.0	6.45	0.255	33.0	6.89	0.245	31.2
	∞	6.18	0.262	34.1	6.18	0.262	34.1	6.18	0.262	34.1

TABLE III

The Membrane Transport Properties η, C, and R_m Computed for Model 2 under the Conditions Shown in Table I

		i = 1 mA/cm²			i = 5 mA/cm²			i = 10 mA/cm²		
$\bar{X}_2$ (M)	n	C (mM)	η	R_m ($\Omega \cdot cm^2$)	C (mM)	η	R_m ($\Omega \cdot cm^2$)	C (mM)	η	R_m ($\Omega \cdot cm^2$)
10^{-2}	2	6.27	2.60	11.9	6.15	2.63	12.0	5.81	2.72	12.5
	10	6.20	2.61	11.9	6.17	2.62	11.9	6.07	2.65	12.0
	∞	6.18	2.62	11.9	6.18	2.62	11.9	6.18	2.62	11.9
10^{-3}	2	9.514	1.105	13.29	9.512	1.105	13.29	9.505	1.105	13.30
	10	9.513	1.105	13.29	9.512	1.105	13.29	9.510	1.105	13.29
	∞	9.512	1.105	13.29	9.512	1.105	13.29	9.512	1.105	13.29

creases with n for low values of $\bar{X}_1$. In the first case, the two membrane layers nearest to the membrane surfaces have a high resistance when compared to that of the membrane core (see model 1 in Fig. 1), so that an increase in the thickness of these layers leads to greater values of R_m. In the second case, just the opposite occurs: the above-mentioned membrane layers now have lower electrical resistances than the membrane core. As the thicknesses of these layers decrease with n, it turns out that R_m increases with n.

Table III shows a rather surprising effect. For small currents (1 mA/cm²), the changes of C, η, and R_m with n and i are found to be similar to those of Table II. However, for higher currents the average coion concentration takes *smaller* values than that of the homogeneous membrane. Likewise, the ratio η *increases* when increasing the membrane inhomogeneity, which is opposite the trend observed previously. (Again, the inhomogeneity effects vanish when $c_0 \gg \bar{X}_2$.) The origin of these new trends for C and η can be seen in Fig. 4. The relatively high electric current (5–10 mA/cm²) modifies the coion concentration profile across the membrane in such a way that for the inhomogeneous case a *better coion exclusion* than that of the homogeneous membrane results. This effect does not appear for small currents, as can be seen by comparing the total areas enclosed under the three coion profiles shown in Fig. 4. In conclusion, we see that the relative importance of the migration transport and the membrane inhomogeneity contributions to the concentration profile (see Eq. [15]) determines the appearance of the new trends. However, the establishment of the exact physical conditions under which the reversal of the effects occurs is a question that deserves more attention.

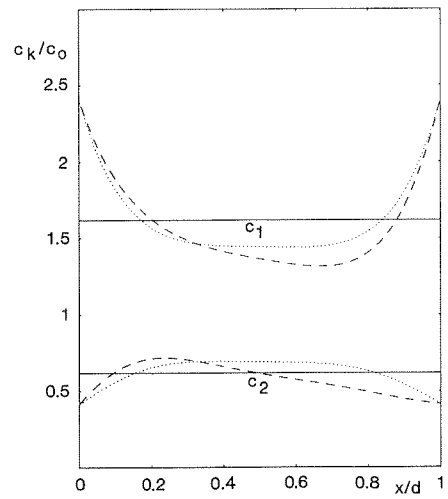

FIG. 4. Dimensionless coion and counterion concentration profiles across the membrane for model 2, case n = 2, $c_0/\bar{X}_2$ = 1. Two different values of current density i are considered: (· · ·) 1 mA/cm²; (---) 10 mA/cm². The continuous plots (—) correspond to the homogeneous case, $n = \infty$.

DISCUSSION

The effects that a macroscopic fixed charge inhomogeneity exerts on some membrane transport properties have been theoretically analyzed. Although we have tried to ensure that our models bear some resemblance to real systems, we must admit that a number of potentially important mechanisms have been left out in order to restrict the theoretical complexity to a reasonable level (1, 2). However, despite the crude nature of some assumptions, certain results may be significant.

Consider first the electric potential profile shown in Fig. 3 for *model 1*. The smooth dependence of ψ on x is perhaps *more realistic* than the abrupt potential jump at the interfaces resulting from the classical Donnan equilibrium relationships (this jump would correspond to the homogeneous membrane, $n = \infty$, in Fig. 3). This continuous dependence of ψ on x results from the fact that $X_1(x)$ also varies in a continuous way from the solution to the membrane core. Note also that model 1 considers the *transport* equations across the *interfacial region* between the bulk solution and the membrane core (where $X_1(x)$ attains a nearly constant value), the classical assumption of a *sharp boundary* between the solution and the homogeneous membrane being now unnecessary. (This classical assumption often involves the use of *equilibrium conditions* at the interface even for high currents i.) Thus, we see that model 1 may be useful not only for a type of inhomogeneous membrane but also for simulating real "homogeneous" membranes having an interfacial region of *finite* thickness over which the physical properties change smoothly from the solution to the membrane core under the influence of transport. (Note that taking the limit $J_k \to 0$ in Eq. [5] leads to the equilibrium relationships characteristic of the abrupt model for the membrane–solution interface (12).) Of course, the thickness of the solution–membrane interfacial region may be in practice much smaller than the total membrane thickness, and this fact would justify the extensive use of the abrupt model for the interface. However, it is well known that some membrane processes such as electrodialysis clearly show the need for more elaborated theories for the above-mentioned interfacial region, especially when the high electric currents cause the polarization effects to become dominant (13).

Tables II and III also show some interesting results. Indeed, we see that a simple redistribution of a constant quantity of fixed charge groups, resulting in a *macroscopic* membrane inhomogeneity, clearly modifies the observed transport properties. Except for model 2 at high currents, the membrane inhomogeneity leads to *poorer* permselectivity values than those computed for the homogeneous case. Reiss and Bassignana have predicted significant current efficiency improvements when studying inhomogeneous three-piece membranes consisting of a thick low-capacity piece sandwiched between two high-capacity pieces (1). Our model 2 bears some resemblance to the discontinuous three-piece membrane described in Ref. (1), and we have also found the above-mentioned behavior here. Thus, when comparing this latter result to those obtained with model 1, we conclude that the predicted changes in the coion exclusion and the current efficiency depend on the particular functional form of the fixed charge distribution considered (see also Ref. (2) in this context).

In conclusion, let us note that a high degree of macroscopic homogeneity is difficult to achieve in practice for many synthetic membranes and might even not be desirable in some specific applications. In addition, there have been reported situations where initially homogeneous membranes have acquired certain macroscopic inhomogeneities due to continuous use. Following the ideas contained in Refs. (1–4), we have studied here the transport across a particular type of inhomogeneous membranes on the basis of very simple but still plausible (3) models. Although particular emphasis has been given to the basic aspects

of membrane transport theory, it is expected that some of the conclusions obtained may also be of interest for practical purposes.

ACKNOWLEDGMENT

This work has been partially sponsored by the Comisión Interministerial de Ciencia y Tecnología, CICYT, Ministry of Education and Science of Spain, under Project PB89-0420.

REFERENCES

1. Reiss, H., and Bassignana, I. C., *J. Membrane Sci.* **11,** 219 (1982).
2. Selvey, C., and Reiss, H., *J. Membrane Sci.* **23,** 11 (1985).
3. Pinéri, M., *in* "Coulombic Interactions in Macromolecular Systems" (A. Eisenberg and F. E. Bailey, Eds.), p. 159. ACS Symp. Ser. No. 302, Amer. Chem. Soc., Washington, DC, 1986.
4. Petropoulos, J. H., *J. Membrane Sci.* **52,** 305 (1990).
5. Larter, R., *J. Membrane Sci.* **28,** 165 (1986).
6. Kuntz, W. H., Larter, R., and Uhegbu, C. E., *J. Amer. Chem. Soc.* **109,** 2582 (1987).
7. Steinmetz, C. G., and Larter, R., *J. Phys. Chem.* **92,** 6113 (1988).
8. Larter, R., *Chem. Rev.* **90,** 355 (1990).
9. Ohshima, H., Makino, K., and Kondo, T., *J. Colloid Interface Sci.* **113,** 369 (1986).
10. Buck, R. P., *J. Membrane Sci.* **17,** 1 (1984).
11. Press, W. H., Flannery, B. P., Tenkolsky, S. A., and Vetterling, W. T., "Numerical Recipes," p. 550. Cambridge Univ. Press, Cambridge, 1984.
12. Manzanares, J. A., Mafé, S., and Pellicer, J., *Ber. Bunsenges. Phys. Chem.* **93,** 37 (1989).
13. Rubinstein, I., Staude, E., and Kedem, O., *Desalination* **69,** 101 (1988).